

Courant Institute of
Mathematical Sciences

AEC Computing and Applied Mathematics Center

A Detached Shock Calculation by
Second Order Finite Differences

Arnold Lapidus

AEC Research and Development Report

Mathematics

February 1967



New York University

NEW YORK UNIVERSITY
COURANT INSTITUTE - LIBRARY
251 Mercer St. New York, N.Y. 10012

UNCLASSIFIED

AEC Computing and Applied Mathematics Center
Courant Institute of Mathematical Sciences
New York University

Mathematics

NYO-1480-69

A DETACHED SHOCK CALCULATION BY SECOND ORDER
FINITE DIFFERENCES

Arnold Lapidus

Contract No. AT(30-1)-1480

UNCLASSIFIED

NEW YORK UNIVERSITY
COURANT INSTITUTE • LIBRARY

Table of Contents

	Page
I. Introduction	1
II. Differential Equations	4
III. Geometry	9
IV. Difference Equations	13
V. Stability: Simplified Lax-Wendroff Artificial Viscosity	32
VI. Computation	37
A. Test Case	37
B. Initial Flow	37
C. Verifications	39
1. Bernoulli Steady State Constant	39
2. Stagnation Point Pressure	40
3. Standoff Distance of the Shock as a Function of Time	40
4. Pressure Profile on the Body	41
5. Final Shape of The Shock	42
6. Summary	42
Graphs	44
Bibliography	49

ABSTRACT

A detached shock problem for a symmetric curved convex cylindrical body moving parallel to its plane of symmetry was solved using a third order accurate Richtmyer form of the Lax-Wendroff conservation equations. One innovation is an easy to use "artificial viscosity" term which preserves the high order of accuracy of the calculation while removing the non-linear instabilities which otherwise appear in the shock region and near boundaries. Another innovation is a simple transformation of Cartesian space which changes the curved body into a straight line, thus reducing the large number of special points and irregularly shaped mesh regions which would otherwise appear in the difference method calculation. Such transformations are shown to preserve the conservation property of the system of differential equations. Other aspects of the third order artificial viscosity term and the transformation are discussed. The results of a numerical calculation on a CDC 6600 Computer are compared to known results.

I. Introduction.

Consider a smooth plane-symmetric convex cylindrical body moving parallel to its axis of symmetry with constant supersonic speed through a perfect compressible gas. A steady state consists of a detached shock at some distance from the body which has a shape which depends on the shape of the body and its speed. There is a region of flow behind the shock and in front of the body in which the flow is subsonic, and a region behind the shock in which the flow is supersonic, these regions being separated by the so called sonic line. The problem which is considered here is to determine the position of the shock near the sonic region and the flow in the sonic region for a specific case in which the steady state configuration looks like Figure 1.

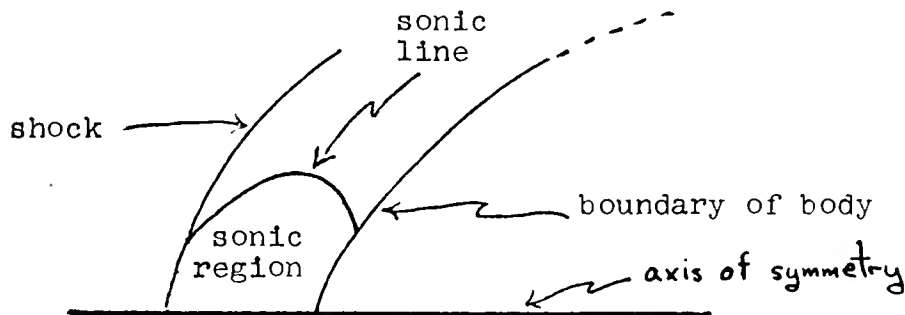


Figure 1.

The detached shock problem has been tackled by diversified and interesting mathematical methods. In the method of lines of Belotserkovskii and Dorodnitsyn [9], the region of interest is divided into strips in which the partial differential equations are reduced to coupled ordinary differential equations that are then solved numerically. The inverse methods [6,7,14] are those in which the position of the shock is assumed to be known and the position of the body is determined. By iterating the shape of the shock, a flow can be found in which the computed shape of the body is close to that of the problem. Van Dyke's method [14] is very fast and accurate. In [7], the constructive method of the Cauchy-Kowalewski theorem is used to obtain very accurate numerical results. Garabedian's interesting method, used in [6], is to continue the flow into the complex plane in order to obtain a hyperbolic initial value problem.

The detached shock problem is also a favorite practice problem for developing, testing and demonstrating time dependent methods as in [3,8,15,16].

In Burstein's work [8] a time dependent flow which tends to the steady state is calculated using conservation equations and the shock is determined as a region of rapid variation of the flow quantities; we proceed similarly. The new features here compared to [8] are:

- (1) A simpler artificial viscosity term is used.
- (2) Since the boundary of the body is a curve instead of a straight line, a transformation of the Cartesian plane is effected which maps the curved body onto a straight vertical line, and the finite difference calculation is carried out in this non-physical coordinate system. The conservation laws are rewritten as conservation laws in this new system.
- (3) To continue calculating near the upper boundary of the mesh, flow quantities are extrapolated from the interior points to the boundary.

Finite difference methods of third order accuracy similar to those in [8] were employed in the computation except near the body and the artificial upper boundary where the methods used were only second order to keep the computation from becoming unstable. The stability and accuracy of the computation will be discussed in the following sections on the differential equations as well as in later sections on the numerical results.

II. Differential Equations.

Fundamental in this approach to solving the detached shock problem is the use of the conservation form [4,5] of the equations of time dependent two dimensional compressible fluid dynamics:

$$(1) \quad \frac{\partial U}{\partial t} + \frac{\partial F(U)}{\partial x} + \frac{\partial G(U)}{\partial y} = 0$$

where

$$U = \begin{bmatrix} \rho \\ m \\ n \\ e \end{bmatrix} \quad F(U) = \begin{bmatrix} m \\ m^2/\rho + p \\ mn/\rho \\ (e+p)m/\rho \end{bmatrix} \quad G(U) = \begin{bmatrix} n \\ mn/\rho \\ n^2/\rho + p \\ (e+p)n/\rho \end{bmatrix}$$

in which

x,y	are cartesian coordinates
t	is time
ρ	is mass per unit volume
u	is the horizontal velocity component
v	is the vertical velocity component
m	is $\rho \cdot u$
n	is $\rho \cdot v$
e	is total energy per unit volume
p	is given by $e = p/(\gamma-1) + \rho(u^2+v^2)/2$
γ	is the ratio of specific heats (we are assuming a gamma-law gas)

In this approach the shock is not a boundary but simply an interior region of rapid variation of the flow quantities. In fact the reason for using the conservation form of the equations is that it includes the shock conditions as well as the differential equations of motion of the gas. Later we will use a transformation of space.

The following theorem shows that if a non-singular transformation of space is made, then any conservation law expressed in the old coordinates can always be rewritten as a conservation law in the new coordinates.

Theorem 1. Under non-singular space transformations, conservation laws are transformed into conservation laws.

Proof: A conservation law is expressed by

$$(2) \quad \int_G U_{\underline{t}} dx + \int_{dG} F_n dS = 0$$

where $F_n = \vec{F} \cdot \vec{n}$, in which \vec{F} is a vector (F_1, \dots, F_m) and $\vec{n} = (n_1, \dots, n_m)$ is the normal to the surface G .

After a change in variables from x_1, \dots, x_m to ξ_1, \dots, ξ_m we want to show that (2) changes into an equation of the same form in the new coordinates. Let

$$J = \partial(x_1, \dots, x_m) / \partial(\xi_1, \dots, \xi_m)$$

and let J_s be the Jacobian for the surface element of (2).

Let M be defined as the matrix which transforms the direction of the normal \vec{v} to the surface in (ξ_1, \dots, ξ_m) space into the direction \vec{n} , of the associated normal to the surface in (x_1, \dots, x_m) space. The integral (2) becomes

$$(3) \quad \int_{\bar{G}} (\bar{U} J)_t d\bar{\xi} + \int_{\partial \bar{G}} (\bar{F} \cdot \vec{n}) J_s d\bar{S} = 0$$

where bars denote the quantities in the new coordinate system. Now

$$(\bar{F} \cdot \vec{n}) J_s = (J_s \cdot \bar{F}, \vec{n}) = (J_s \bar{F}, M \cdot \vec{v}) = (M^T J_s \bar{F}, \vec{v})$$

where M^T means transpose of M . This shows that $(\bar{F} \cdot \vec{n}) J_s$ is the component of a vector normal to \bar{S} and therefore (2) and (3) are of the same form. Q.E.D.

A practical way to determine the components of the flux is given by the following. Use the differential form (1) of the conservation laws. Using the chain rule and multiplying (1) by J we get

$$(3a) \quad (J \bar{U})_t + \left(\sum_{j=1}^m \sum_{k=1}^m \frac{\partial \bar{F}_j}{\partial \xi_k} \frac{\partial \xi_k}{\partial x_j} \right) J = 0 .$$

According to the theorem, the spatial part of (3a) is in conservation form; it is not hard to show that it is

$$(3b) \quad (J \bar{U})_t + \sum_{k=1}^n \left(\sum_{j=1}^m J \bar{F}_j \frac{\partial \xi_k}{\partial x_j} \right)_{\xi_k} = 0 .$$

It is amusing that the validity of (3b) follows from the conceptual argument presented. Of course, (3b) can also be verified by a computation. We note that (3a) can be written as

$$(J \bar{U})_t + \sum_{j=1}^n \frac{\partial(x_1, \dots, x_{j-1}, \bar{F}_j, x_{j+1}, \dots, x_m)}{\partial(\xi_1, \dots, \xi_n)} .$$

But according to a theorem of advanced calculus [13] $\frac{\partial(x_1, \dots, x_{j-1}, \bar{F}_j, x_{j+1}, \dots, x_m)}{\partial(\xi_1, \dots, \xi_n)}$ is of the form $\sum (p_k)_{\xi_k}$ [13].

Specifically, the transformation which we used was

$$(4) \quad \xi_1 = x/h(y) \quad \xi_2 = y \quad \text{in which } h'(y) \text{ exists and } h(y) \neq 0.$$

This changes the fundamental equation (1) into

$$(5) \quad (h(\xi_2)U)_t + (f-h'(\xi_2) \cdot \xi_1 g_1)_{\xi_1} + (gh)_{\xi_2} = 0 ,$$

and maps the curve $x = h(y)$ into the line $\xi_1 = 1$. In this problem the curve $x = h(y)$ is the boundary of the body.

Such a transformation of the space of independent variables is employed as a means of simplifying computation near the body. It is obvious from Theorem 1 [eq. (3b)] that the transformation does not affect the existence of the shock or its position.

In summary, we've shown that the conservation properties of the system are preserved under the transformation and that the essential properties of the shock are also preserved under the transformation. It is also obvious that if the function h satisfies the symmetry property $h(y) = h(-y)$ then the symmetry of the solution to the transformed system is also preserved.

III. Geometry.

The exterior of the obstacle in which the flow takes place is unbounded. Since only a finite number of lattice points can be employed in any actual computation, the neighborhood of infinity has to be dealt with in some summary fashion. In this work, we resort to the simple and crude expedient of confining the calculation to a finite region of the flow field which contains the whole sonic regime.

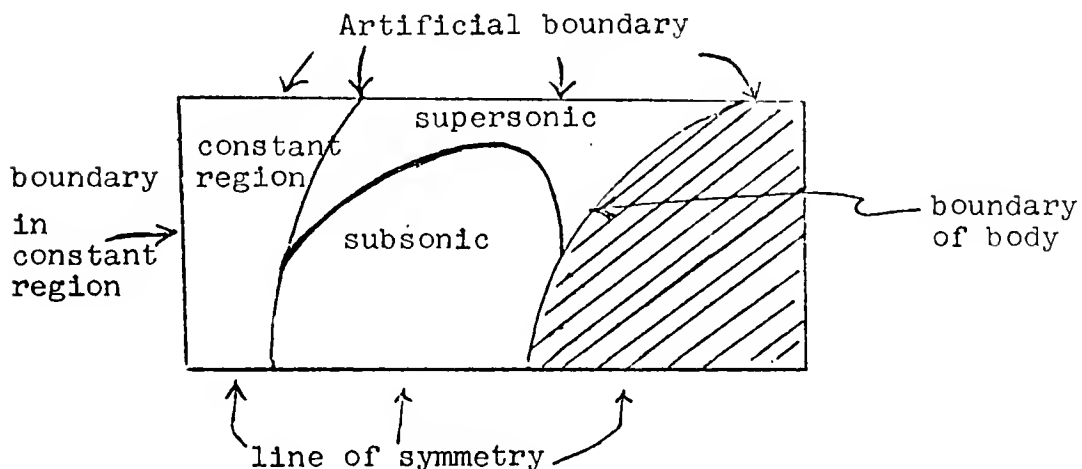


Figure 2.

In this approach the region is bounded from above by an artificial boundary line on which boundary conditions have to be imposed which approximate well the state of affairs along this line in the true solution. At any rate, the error incurred by imposing artificial boundary conditions should be comparable to discretization errors.

The remaining geometrical inconvenience is the incommensurability of a curved body with a rectangular mesh. We solved that problem by mapping the irregularly shaped cut out configuration onto a rectangular region by a transformation which took the boundary of the body into the right side of a rectangle. The mapping which we used was

$$\xi_1 = x/h(y) \quad \xi_2 = y \quad \text{where } x = h(y) \text{ is the function}$$

which traces out the boundary of the body and is assumed to be continuously differentiable, symmetric in y and non-vanishing. Then the Jacobian of the transformation is also non-vanishing.

Choose the coordinates so that the left boundary of Figure 2 is the line $x = 0$; then its image is the line $\xi_1 = 0$. The lines $y = 0$ and $y = .2$ are transformed into

$\xi_2 = 0$ and $\xi_2 = .2$, while the curve $x = h(y)$ gets transformed into the line $\xi_1 = 1$. Figure 3 illustrates the new configuration in which the three previously straight boundaries remain so while the curved body is transformed into a line.

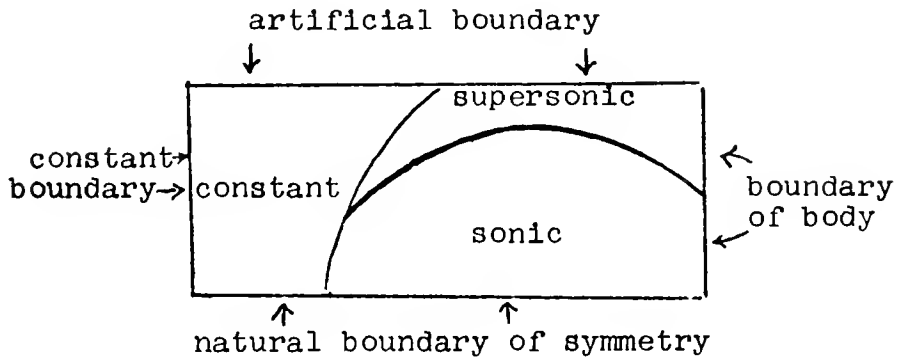


Figure 3.

This transformation also saves some computer space because the region behind the body, the shaded space in Figure 2, has been eliminated.

The mesh which was chosen for the machine computation is a 79 x 20 rectangular grid projected onto that

rectangular portion of $\xi_1\xi_2$ space given by $[0,1] \times [0,y_{\max}]$. It is the set of points $(j\Delta\xi_1, k\Delta\xi_2)$ with $j = 0, \dots, 78$; $k = 0, \dots, 19$ and $\Delta\xi_1 = 1/78$, $\Delta\xi_2 = y_{\max}/19$. The body is denoted by the right sided boundary of the mesh since the boundary of the body is transformed into the line $\xi_1 = 1$. The shock is not introduced as an explicit boundary but is determined as the locus of the most rapid change in the values of appropriate flow quantities.

In summary, a region of interest is cut out of the plane and then transformed into a rectangle. The rectangular region is then represented as a rectangular mesh which can be used in a machine computation.

IV. Difference Equations.

In this section, a difference scheme for the fundamental equation (1) which is similar to that in [4] is described and is shown to be consistent and to have truncation error $O(\Delta^3)$ in the smooth part of the flow which is far from shocks, body or other boundaries. We hoped that no special methods would have to be used at the shock except to use the two step scheme and that the location of the shock could be determined by sharp variations in some of the flow quantities such as density, entropy or pressure. The main reason for this is that the two step scheme is itself conservative as shown by Lax and Wendroff in [5]. That is, solutions U of the two step equations satisfy a discrete analogue of the integral relation

$$(6) \quad \iiint (w_t U + w_x F(U) + w_y G(U)) \, dx \, dy \, dt = 0 ,$$

where $w(x,y,t)$ is a differentiable function of compact support. Such difference schemes are conjectured to satisfy the entropy condition. The first step of the two step scheme is:

$$\begin{aligned}
 U_{j+\frac{1}{2}, k+\frac{1}{2}}^{n+\frac{1}{2}} &= \frac{1}{4} (U_{jk}^n + U_{j+1, k}^n + U_{jk+1}^n + U_{j+1, k+1}^n) \\
 (7a) \quad & - \frac{\Delta t}{2\Delta x} (F_{j+1, k+\frac{1}{2}}^n - F_{j, k+\frac{1}{2}}^n) - \frac{\Delta t}{2\Delta y} (G_{j+\frac{1}{2}, k+1}^n - G_{j+\frac{1}{2}, k}^n).
 \end{aligned}$$

The second step of the scheme is:

$$(7b) \quad U_{jk}^{n+1} = U_{jk}^n - \frac{\Delta t}{\Delta x} (\bar{F}_{j+\frac{1}{2}, k}^{n+\frac{1}{2}} - \bar{F}_{j-\frac{1}{2}, k}^{n+\frac{1}{2}}) - \frac{\Delta t}{\Delta y} (\bar{G}_{j, k+\frac{1}{2}}^{n+\frac{1}{2}} - \bar{G}_{j, k-\frac{1}{2}}^{n+\frac{1}{2}})$$

in which

$$(7c) \quad U_{jk}^n = \begin{bmatrix} \rho_{jk}^n \\ m_{jk}^n \\ n_{jk}^n \\ e_{jk}^n \end{bmatrix}, \quad F_{jk}^n = \begin{bmatrix} m_{jk}^n \\ (m_{jk}^n)^2 / \rho_{jk}^n + p_{jk}^n \\ m_{jk}^n \cdot n_{jk}^n / \rho_{jk}^n \\ (e_{jk}^n + p_{jk}^n) \cdot m_{jk}^n / \rho_{jk}^n \end{bmatrix}, \quad G_{jk}^n = \begin{bmatrix} n_{jk}^n \\ m_{jk}^n \cdot n_{jk}^n / \rho_{jk}^n \\ (n_{jk}^n)^2 / \rho_{jk}^n + p_{jk}^n \\ (e_{jk}^n + p_{jk}^n) n_{jk}^n / \rho_{jk}^n \end{bmatrix}$$

and

$$\begin{aligned}
 \bar{F}_{j+\frac{1}{2}, k}^{n+\frac{1}{2}} &= (F_{j+\frac{1}{2}, k+\frac{1}{2}}^{n+\frac{1}{2}} + F_{j+\frac{1}{2}, k-\frac{1}{2}}^{n+\frac{1}{2}}) / 2; \\
 (7d) \quad \bar{G}_{j, k+\frac{1}{2}}^{n+\frac{1}{2}} &= (G_{j+\frac{1}{2}, k+\frac{1}{2}}^{n+\frac{1}{2}} + G_{j-\frac{1}{2}, k+\frac{1}{2}}^{n+\frac{1}{2}}) / 2.
 \end{aligned}$$

This is a nine point scheme in the sense that only nine points of the mesh at time $n \cdot \Delta t$ are needed to obtain numerical values at a point at time $(n+1)\Delta t$. However, four

additional points (A,B,C,D of Figure 4) are used for the computation of intermediate values. This scheme can be used only for points which have all eight neighbors.

Next we want to prove consistency for this scheme (equations (7)) and also that the discretization error is $O(\Delta^3)$.

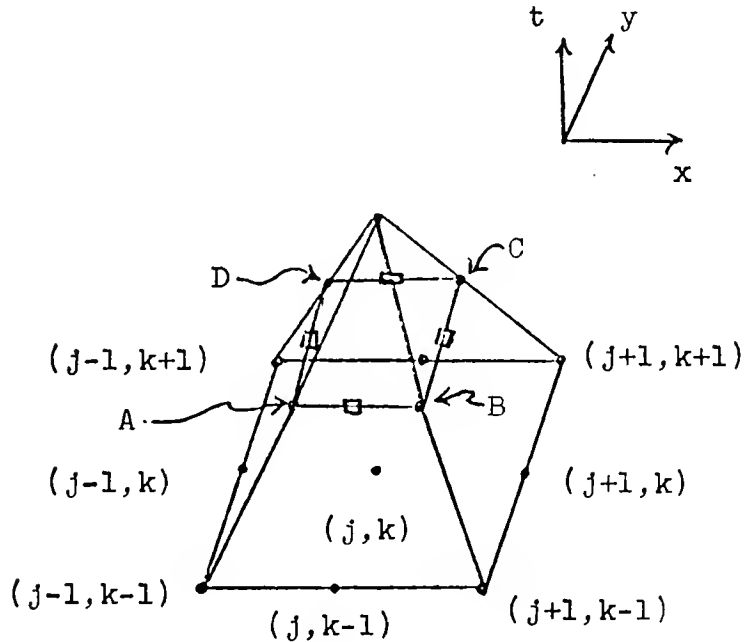


Figure 4.

Let the truncation error at a point be defined as the difference between a computed solution and the true solution having the same initial data. This is also called

discretization error.

Theorem 2. The scheme described by formulas (7) is consistent with the fundamental equation (1) and has a truncation error which is $O(\Delta^3)$ in the smooth part of the flow.

Proof: Define the operators $N(U)$ and $N_\Delta(U)$ by the equations

$$N(U) = U_t + F_x + G_y$$

and

$$\begin{aligned} N_\Delta(U) = & (U_{jk}^{n+1} - U_{jk}^n)/\Delta t + (\bar{F}_{j+\frac{1}{2}k}^{n+\frac{1}{2}} - \bar{F}_{j-\frac{1}{2}k}^{n+\frac{1}{2}})/\Delta x + \\ & + (\bar{G}_{jk+\frac{1}{2}}^{n+\frac{1}{2}} - \bar{G}_{jk-\frac{1}{2}}^{n+\frac{1}{2}})/\Delta y. \end{aligned}$$

In order to prove the consistency of the operators N and N_Δ it will be shown that

$$\lim_{\Delta \rightarrow 0} |N^{n+\frac{1}{2}}(U) - N_\Delta^{n+\frac{1}{2}}(U)| = 0$$

for arbitrary smooth functions U . First we assume that

$$(8a) \quad (\bar{F}_{j+\frac{1}{2}k}^{n+\frac{1}{2}} - \bar{F}_{j-\frac{1}{2}k}^{n+\frac{1}{2}})/\Delta x = F_x(U_{jk}^{n+\frac{1}{2}}) + O(\Delta)$$

and

$$(8b) \quad (\bar{G}_{jk+\frac{1}{2}}^{n+\frac{1}{2}} - \bar{G}_{jk-\frac{1}{2}}^{n+\frac{1}{2}})/\Delta y = G_y(U_{jk}^{n+\frac{1}{2}}) + O(\Delta)$$

in which quantities on the left are evaluated by the difference scheme and the quantities on the right are evaluated by the assumed known function U . Then we have

$$\begin{aligned} |N^{n+\frac{1}{2}} U - N_{\Delta}^{n+\frac{1}{2}} U| &= |U_t^{n+\frac{1}{2}} + F_x^{n+\frac{1}{2}} + G_y^{n+\frac{1}{2}} - \frac{U_{jk}^{n+1} - U_{jk}^n}{\Delta t} \\ &\quad - F_x^{n+\frac{1}{2}} - G_y^{n+\frac{1}{2}} + O(\Delta)| = |U_t^{n+\frac{1}{2}} - U_t^{n+\frac{1}{2}} + O(\Delta)| = |O(\Delta)| \end{aligned}$$

which goes to 0 as $\Delta \rightarrow 0$.

Now we still have to prove (8a) and (8b). The proof is complicated by the fact that the approximations to the derivatives in the difference scheme have an intermediate step. Only the proof of (8a) follows. The proof of (8b) would follow similar lines. To make the proof a little clearer, the function values which are computed from the difference scheme are denoted by V 's. Then

$$\begin{aligned} (7d) \quad \bar{F}_{j+\frac{1}{2}, k}^{n+\frac{1}{2}} &= (F(V_{j+\frac{1}{2}, k+\frac{1}{2}}^{n+\frac{1}{2}}) + F(V_{j+\frac{1}{2}, k-\frac{1}{2}}^{n+\frac{1}{2}}))/2 \\ (9) \quad F(V_{j+\frac{1}{2}, k+\frac{1}{2}}^{n+\frac{1}{2}}) &= \bar{F}(U_{jk}^n, U_{j+1, k}^n, U_{j, k+1}^n, U_{j+1, k+1}^n) \end{aligned}$$

where \bar{F} is a very smooth function of $U_{jk}^n, U_{j+1, k}^n, \dots$.

We are assuming that U is a smooth function of x, y and t

so

$$(10) \quad F(V_{j+\frac{1}{2}, k+\frac{1}{2}}^{n+\frac{1}{2}}) = P(\Delta x, \Delta y) \quad \text{where } P \text{ is a smooth function of } \Delta x \text{ and } \Delta y$$

and

$$(11) \quad P(\Delta x, \Delta y) = P(0,0) + P_1(0,0)\Delta x + P_2(0,0)\Delta y + P_{11}(0,0)\frac{\Delta x^2}{2} \\ + P_{12}(0,0)\Delta x \Delta y + P_{22}(0,0)\frac{\Delta y^2}{2} + o(\Delta^3) .$$

Then by (7d) and (11) we obtain

$$(12) \quad \frac{\bar{F}_{j+\frac{1}{2},k}^{n+\frac{1}{2}} - \bar{F}_{j-\frac{1}{2},k}^{n+\frac{1}{2}}}{\Delta x} = \frac{F(V_{j+\frac{1}{2},k+\frac{1}{2}}^{n+\frac{1}{2}}) + F(V_{j+\frac{1}{2},k-\frac{1}{2}}^{n+\frac{1}{2}})}{2\Delta x} \\ - \frac{F(V_{j-\frac{1}{2},k+\frac{1}{2}}^{n+\frac{1}{2}}) + F(V_{j-\frac{1}{2},k-\frac{1}{2}}^{n+\frac{1}{2}})}{2\Delta x} = 2P_1(0,0) + o(\Delta x^2) .$$

Next, we will show that $2P_1(0,0) = F_x(x,y,t) + o(\Delta t)$ which will finish the proof of consistency. From (9) and (7a)

$$(13) \quad P(\Delta x, \Delta y) = F(\frac{1}{4}(U(x,y,t) + U(x+\Delta x,y,t) + U(x,y+\Delta y,t) \\ + U(x+\Delta x,y+\Delta y,t))) - (\Delta t/2\Delta x)(F(U(x+\Delta x,y,t)) \\ - F(U(x,y,t))) - \Delta t/2\Delta y \cdot (G(U(x,y+\Delta y,t)) - G(U(x,y,t))) .$$

Then by differentiating (13) with respect to Δx we get

$$(14) \quad P_1(\Delta x, 0) = F_U \cdot \\ \cdot [U_x/2 - \Delta t/2\Delta x \cdot (F_U U_x - [F(U(x+\Delta x,y,t)) - F(U(x,y,t))]/\Delta x)]$$

and for $\Delta x \rightarrow 0$

$$P_1(0,0) = F_U \cdot [U_x/2 - F_{xx}\Delta t/4] = F_x(x,y,t)/2 + O(\Delta t).$$

This completes the proof of consistency.

Now we will show that the discretization error in the smooth part of the flow is $O(\Delta^3)$. Let the solution of the differential equation be $U(x,y,t)$ and let the result of calculating the approximation to the solution at time $t+\Delta t$ from values of the solution at time t be denoted by v_{jk}^{n+1} . We want to show

$$(15) \quad U(x,y,t+\Delta t) - v_{jk}^{n+1} = O(\Delta^3) .$$

From the differential equation we get that

$$(16) \quad U(x,y,t+\Delta t) = U(x,y,t) - \Delta t(F_x(x,t,t+\Delta t/2) + G_y(x,y,t+\Delta t/2)) + O(\Delta^3)$$

and from the difference scheme

$$(17) \quad v_{jk}^{n+1} = U(x,y,t) - \frac{\Delta t}{\Delta x} \left(\bar{F}_{j+\frac{1}{2}k}^{n+\frac{1}{2}} - \bar{F}_{j-\frac{1}{2}k}^{n+\frac{1}{2}} \right) - \frac{\Delta t}{\Delta y} \left(\bar{G}_{jk+\frac{1}{2}}^{n+\frac{1}{2}} - \bar{G}_{jk-\frac{1}{2}}^{n+\frac{1}{2}} \right)$$

where \bar{F} and \bar{G} are given by equation (7d). From (17) it is clear that equation (15) will be satisfied if

$$(18) \quad (\bar{F}_{j+\frac{1}{2}k}^{n+\frac{1}{2}} - \bar{F}_{j-\frac{1}{2}k}^{n+\frac{1}{2}})/\Delta x = F_x(x,y,t+\Delta t/2) + O(\Delta^2) ,$$

and similarly for the term in $G(V)$. To prove this, define $P(\Delta x, \Delta y)$ so that

$$F(V_{j+\frac{1}{2}, k+\frac{1}{2}}^{n+1}) = P(\Delta x, \Delta y) =$$

$$(19) \quad \left[\begin{aligned} & (U(x, y, t) + U(x+\Delta x, y, t) + U(x, y+\Delta y, t) + U(x+\Delta x, y+\Delta y, t)) / 4 \\ & - \frac{\Delta t}{2\Delta x} \left(\frac{F(x+\Delta x, y, t) + F(x+\Delta x, y+\Delta y, t)}{2} - \frac{F(x, y, t) + F(x, y+\Delta y, t)}{2} \right) \\ & - \frac{\Delta t}{2\Delta y} \left(\frac{G(x, y+\Delta y, t) + G(x+\Delta x, y+\Delta y, t)}{2} - \frac{G(x, y, t) + G(x+\Delta x, y, t)}{2} \right) \end{aligned} \right]$$

From (19) it is clear that the equations

$$(20) \quad F(V_{j-\frac{1}{2}, k+\frac{1}{2}}^{n+\frac{1}{2}}) = P(-\Delta x, \Delta y); \quad F(V_{j+\frac{1}{2}, k-\frac{1}{2}}^{n+\frac{1}{2}}) = P(\Delta x, -\Delta y);$$

$$F(V_{j-\frac{1}{2}, k-\frac{1}{2}}^{n+\frac{1}{2}}) = P(-\Delta x, -\Delta y)$$

hold. If we assume that $U(x, y, t)$ is sufficiently smooth, we can expand P as

$$(21) \quad \begin{aligned} P(\Delta x, \Delta y) &= P(0, 0) + P_1(0, 0)\Delta x + P_2(0, 0)\Delta y \\ &\quad + P_{11}(0, 0)\Delta x^2/2 + P_{12}(0, 0)\Delta x \Delta y + \\ &\quad + P_{22}(0, 0)\Delta y^2/2 + o(\Delta^3). \end{aligned}$$

From (20) and (21) it then follows that

$$(22) \quad [F(V_{j+\frac{1}{2}, k+\frac{1}{2}}^{n+\frac{1}{2}}) + F(V_{j+\frac{1}{2}, k-\frac{1}{2}}^{n+\frac{1}{2}})]/2\Delta x - \\ - [F(V_{j-\frac{1}{2}, k+\frac{1}{2}}^{n+\frac{1}{2}}) + F(V_{j-\frac{1}{2}, k-\frac{1}{2}}^{n+\frac{1}{2}})]/2\Delta x = 2P_1(0,0) + O(\Delta^2).$$

We will now show that

$$(23) \quad P_1(0,0) = F_x(x,y,t+\Delta t/2)/2 + O(\Delta^2)$$

and then (22) implies (18). That is, it is sufficient to show (23) in order to show that the discretization error is $O(\Delta^3)$.

To show (23), we differentiate (19) with respect to Δx and obtain

$$P_1(0,0) = \lim_{\substack{\Delta x \rightarrow 0 \\ \Delta y \rightarrow 0}} F_U(U(x,y,t) - \Delta t/2 (F_x + G_y)) \cdot [U_x(x,y,t)/2 - \\ - \frac{\Delta t}{2\Delta x} (F_x(x+\Delta x, y, t)) + \frac{\Delta t}{2\Delta x} (\frac{F(x+\Delta x, y, t) - F(x, y, t)}{\Delta x}) - \frac{\Delta t}{2} \frac{G_{xy}}{2}].$$

Then using the hypothesis that $U(x,y,t)$ is a solution to the fundamental equation, we get

$$\begin{aligned}
P_1(0,0) &= F_U(U(x,y,t+\Delta t/2)) \cdot \frac{1}{2} [U_x(x,y,t) + \Delta t/2 (U_t)_x] + O(\Delta^2) \\
&= F_U(U(x,y,t+\Delta t/2))/2 \cdot U_x(x,y,t+\Delta t/2) + O(\Delta^2) \\
&= F_x(x,y,t+\Delta t/2)/2 + O(\Delta^2). \quad \text{Q.E.D.}
\end{aligned}$$

We have now proven that this nine point difference scheme is consistent with the fundamental equation (1) and has truncation error $O(\Delta^3)$ in the interior parts of the mesh which are not in the shock region. The left boundary has constant values and those at the axis of symmetry are computed by reflection. We still have to describe the difference schemes which are applied at the two non trivial boundaries: the body and the upper artificial boundary.

At the upper boundary the flow quantities were evaluated by linear extrapolation as follows:

$$(24) \quad U_{jk}^{n+1} = 2 U_{j-1, k-1}^{n+1} - U_{j-2, k-2}^{n+1}.$$

If the Mach cone at every point of the upper boundary were to leave the rectangular region of calculation, the errors introduced by extrapolation (24) would not affect the accuracy of the computation. While the Mach cones do not leave the region, the curves which are the envelopes of Mach cones starting at the artificial boundary end at points on the body which are still in

the supersonic region. The numerical experiments show that errors which are introduced at the upper boundary affect the subsonic region only slightly. The linear extrapolation (24) is in a 45° degree direction which was roughly the same as that of the nearby characteristics. Scheme (24) was unstable at the early stages of calculation and therefore was replaced by (25) where the factor r was only gradually built up to 1.

$$(25) \quad U_{jk}^{n+1} = U_{j-1 \ k-1}^{n+1} + r \cdot (U_{j-1 \ k-1}^{n+1} - U_{j-2 \ k-2}^{n+1})$$

in which

$r = .5$	if the number of cycles was less than 100 and > 0									
$r = .6$	"	"	"	"	"	"	"	"	200	" " 99
$r = .7$	"	"	"	"	"	"	"	"	300	" " 199
$r = .8$	"	"	"	"	"	"	"	"	400	" " 299
$r = .9$	"	"	"	"	"	"	"	"	500	" " 399
$r = 1.0$	"	"	"	"	"	"	"	"	∞	" " 499

The top point of the body is also treated in this ad hoc fashion of a point on the upper boundary but the other points of the body are treated in a manner which is very much in the spirit of the conservation law approach. To explain the scheme used at the body we will refer to Figure 5.

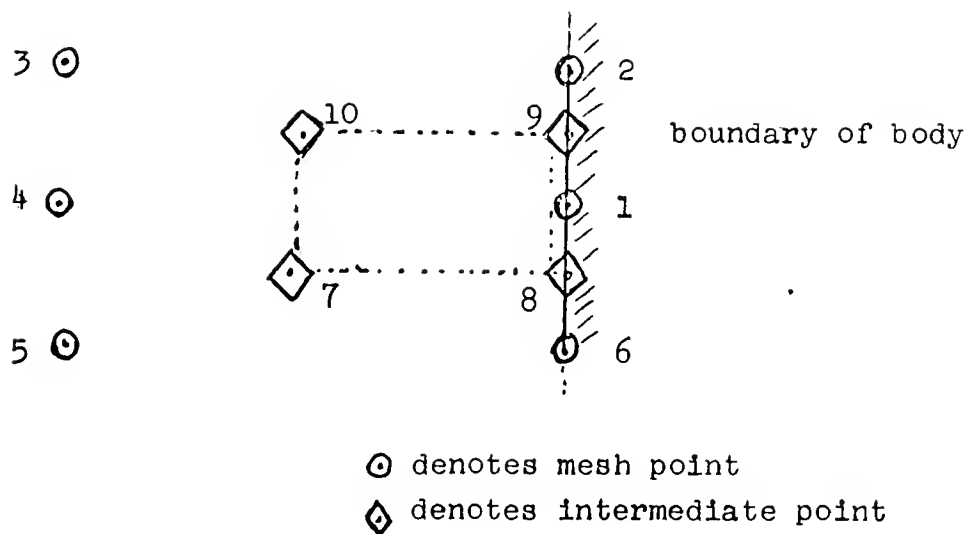


Figure 5. Difference Scheme at the Body.

The flow quantities are assumed to be known at the points labelled 1, 2, 3, 4, 5 and 6 at time t . The problem is to obtain values of the flow quantities for the point labelled 1 at time $t + \Delta t$.

We think of the flow quantities at point 1 as being affected only by the fluxes F and G across the dotted lines. To obtain good estimates of F and G across those lines we first make estimates of the flow quantities at the points labelled 7, 8, 9, 10 at time $t + \Delta t/2$.

At 7 (and 10) we calculate as at ordinary intermediate points. That is, for the point 7 we consider the rectangle whose vertices are the points 1,4,5,6. To compute the change in the flow quantities at point 7, we compute the sum of the fluxes through the sides of the rectangle and add it to the flow quantities. At time t , the average of the flow quantities at points 1,4,5 and 6 was used as an estimate for the values at point 7.

A point such as 8 (or 9) has to be treated in a special way. The method chosen is to estimate its flow quantities at time t by averaging those at points 1 and 6. Since point 8 is in the same large rectangle (1,4,5,6) as point 7, the change in the flow quantities due to fluxes is taken to be the same as at 7.

Having computed the flow quantities at time $t+\Delta t/2$ for the points 7,8,9,10 we use these values to compute the flux across the dotted lines to give the change in the value of the flow quantities at point 1 between time t and $t+\Delta t$. The formulas which follow express the various quantities involved in the procedure described above.

$$\begin{aligned}
 (26a) \text{ Flux into rectangle } (1,4,5,6) &= B_{78} \\
 &= -\frac{\Delta t}{2\Delta x} ((F_6^n + F_1^n)/2 - (F_4^n + F_5^n)/2) \cdot T_1(y) \\
 &\quad - \frac{\Delta t}{2\Delta x} ((G_6^n + G_1^n)/2 - (G_4^n + G_5^n)/2) \cdot T_2(x,y) \\
 &\quad - \frac{\Delta t}{2\Delta y} ((G_1^n + G_4^n)/2 - (G_5^n + G_6^n)/2)
 \end{aligned}$$

$$(26b) \quad v_7^{n+\frac{1}{2}} = \frac{1}{4} (U_1^n + U_4^n + U_5^n + U_6^n) + B_{78}^{n+\frac{1}{2}}$$

$$(26c) \quad v_8^{n+\frac{1}{2}} = \frac{1}{2} (U_1^n + U_6^n) + B_{78}^{n+\frac{1}{2}}$$

where $T_1(y) = 1/h(y)$ $T_2(x,y) = -xh'(y)/h(y)$.

The same formulas with the appropriate changes in subscripts (referring to points in the figure) are used to obtain intermediate values at the points numbered 9 and 10. At the point numbered 1 the difference formula is:

$$(27) \quad \begin{aligned} U_1^{n+1} = & U_1^n - \frac{2\Delta t}{\Delta x} ((F_9^{n+\frac{1}{2}} + F_8^{n+\frac{1}{2}})/2 - (F_7^{n+\frac{1}{2}} + F_{10}^{n+\frac{1}{2}})/2) \cdot T_1(y) \\ & - T_2(x,y) (\frac{2\Delta t}{\Delta x}) ((G_9^{n+\frac{1}{2}} + G_8^{n+\frac{1}{2}})/2 - (G_7^{n+\frac{1}{2}} + G_{10}^{n+\frac{1}{2}})/2) \\ & - (\frac{2\Delta t}{\Delta y}) ((G_9 + G_{10})/2 - (G_8 + G_7)/2) . \end{aligned}$$

This difference scheme is consistent but has an error of second order rather than a third order error as at ordinary points.

The physical boundary condition is that the flow should be parallel to the wall at body points. This was not used so far; we impose it now by replacing the momentum vector calculated at boundary points by one which has the same magnitude and the right direction. Denoting by m' and n' the new momenta, we have

$$(28) \quad \omega = \sqrt{(m^{n+1})^2 + (n^{n+1})^2}$$

$$\omega\eta \rightarrow m^{n+1} \quad - \omega\xi \rightarrow n^{n+1}$$

where (ξ, η) are the components of the normal to the body at the point.

At the nose of the body, the symmetry of the configuration is used to reduce the point to an ordinary point of the body. This is the same procedure used at other points of the axis of symmetry, i.e. the point is reduced to a known type by continuing the flow so that the point gets its full complement of neighbors.

We have now explained the difference method used in the mesh and at boundaries and also discussed the consistency truncation error of the equations. The transformed equations were used in the conservation form as well as in the (analytically) equivalent form:

$$(29) \quad U_t + F_x \cdot h^{-1}(y) - x \cdot G_x \cdot h'(y) \cdot h^{-1}(y) + G_y = 0.$$

A natural question to ask is whether the divergence free conservation form of the equations would be more suitable for computing than the equivalent form (29). To investigate this question the now classical equation

$$(30) \quad U_t + (U^2/2)_x = 0$$

was used. The problem chosen for experimentation was to solve

$$(31) \quad U_t + (U^2/2)_x = 0 \quad \text{on } x \in [-\pi/4, \pi/4], \quad t \in [0, \pi/2],$$

with initial conditions

$$(32) \quad \begin{aligned} U(x, 0) &= 1 \quad \text{for } x < 0 \\ U(x, 0) &= 0 \quad \text{for } x > 0. \end{aligned}$$

The solution to (31) and (32) is

$$(33) \quad \begin{aligned} U(x, t) &= 1 \quad \text{if } x < t/2, \quad 0 < t < \pi/2; \\ U(x, t) &= 0 \quad \text{if } x > t/2. \end{aligned}$$

We now consider a change in the space variable given by

$$(34) \quad \xi = \sin x, \quad -\pi/4 \leq x \leq \pi/4, \quad (-\sqrt{2}/2 \leq \xi \leq \sqrt{2}/2).$$

The transformed function $\bar{U}(\xi, t)$ is then to have initial conditions

$$(35) \quad \begin{aligned} \bar{U}(\xi, 0) &= 1 \quad \text{for } \xi < 0 \\ \bar{U}(\xi, 0) &= 0 \quad \text{for } \xi > 0 \end{aligned}$$

and it will then satisfy

$$\bar{U}_t + (\bar{U}^2/2)_{\xi_x} = 0$$

where

$$\xi_x = \cos x = \sqrt{1 - \sin^2 x} = \sqrt{1 - \xi^2}.$$

Dropping the bar and denoting $(1-\xi^2)^{1/2}$ by T , the problem in the new variable becomes

$$(36) \quad U_t + (U^2/2)_\xi T = 0$$

with

$$U(\xi, 0) = 1 \quad \text{for } \xi < 0$$

and

$$U(\xi, 0) = 0 \quad \text{for } \xi > 0.$$

The solution will then be

$$U(\xi, t) = 1 \quad \text{for } \arcsin \xi < t/2,$$

$$U(\xi, t) = 0 \quad \text{for } \arcsin \xi > t/2.$$

Now let $U/T = V$; then the problem becomes

$$(37) \quad V_t + (T^2 V^2/2)_\xi = 0$$

with

$$V(\xi, 0) = 1/T \quad \text{for } \xi < 0$$

and

$$V(\xi, 0) = 0 \quad \text{for } \xi > 0.$$

The solution is

$$V(\xi, t) = 1/T \quad \text{for } \arcsin \xi < t/2,$$

$$V(\xi, t) = 0 \quad \text{for } \arcsin \xi > t/2.$$

Equation (37) is in conservation form while (36) is not. The pertinent question is whether there is any difference in the results of using a reasonable difference approximation for these.

The difference equations used where

$$(38) \quad U_j^{n+1} = (U_{j+1}^n + U_{j-1}^n)/2 - \frac{1}{4} \frac{\Delta t}{\Delta \xi} ((U_{j+1}^n)^2 - (U_{j-1}^n)^2) T(\xi)$$

$$(39) \quad V_j^{n+1} = (V_{j+1}^n + V_{j-1}^n)/2 - \frac{1}{4} \frac{\Delta t}{\Delta \xi} ((V_{j+1}^n)^2 T_{j+1} - (V_{j-1}^n)^2 T_{j-1}).$$

The results showed that (38) gave five place accuracy except in the shock region while (39) gave only three place accuracy. The reason for this difference is that U is constant while V is not, therefore the error committed by taking the average in the first term on the right is negligible in (38) and appreciable in (39).

Schemes (38) and (39) both had second order accuracy. For third order accurate schemes analogous to the two step method in two dimensions, computational experiments showed almost no difference in the numerical results. The difference analogue of (29) was used as well as the analogue of (5) for the fluid dynamics equations in two dimensions. The results indicate that (5) gives much better accuracy for these equations than (29) does.

In this chapter we discussed the difference equations used far from boundaries and their consistency and

truncation errors. We also discussed the methods at the upper artificial boundary and at the body. The results of a computational experiment for a one dimensional problem justified trying a slightly different form of the difference equations. Stability will be discussed in the next chapter and results of a machine computation will be analyzed in the last chapter.

V. Stability: Simplified Lax-Wendroff Artificial Viscosity.

The major difficulty in this problem was maintaining numerical stability. At various times instabilities appeared near the body, near the shock and at the upper boundary. To counteract this instability we introduced a new type of stabilizing transformation which consisted of replacing the flow quantities U^{n+1} calculated in the last section by new ones U'^{n+1} obtained by smoothing first in the ξ_1 direction and then in the ξ_2 direction according to the following prescription.

$$(40a) \quad U'_{jk}{}^{n+1} = U_{jk}{}^{n+1} + \lambda C \cdot \Delta' (|\Delta' u_{j+1 \ k}^{n+1}| \cdot \Delta' (U_{j+1 \ k}^{n+1}))$$

$$(40b) \quad U''_{jk}{}^{n+1} = U'_{jk}{}^{n+1} + \lambda C \cdot \Delta'' (|\Delta'' v'_{j+1 \ k}{}^{n+1}| \cdot \Delta'' (U'_{j+1 \ k}{}^{n+1}))$$

where $\Delta' U_{jk} = U_{jk} - U_{j-1 \ k}$; $\Delta'' U_{jk} = U_{jk} - U_{jk-1}$ and C is a constant (taken as 4. in actual computations) while u and v' are horizontal and vertical fluid velocity components.

Equation (40a,b) are fractional steps [20] for the numerical solution of the diffusion equation

$$U_t = \lambda C (\Delta^3) [(|u_{\xi_1}| U_{\xi_1})_{\xi_1} + (|v'_{\xi_2}| U_{\xi_2})_{\xi_2}].$$

From this equation it is clear that smoothing is of third order and consequently does not affect the truncation error

of the difference scheme.

Adding such a term to the equations of motion is similar to the von Neumann-Richtmyer approach used in [18] and was motivated by the higher order artificial viscosity of Lax and Wendroff [5].

In [5] Lax and Wendroff introduced a class of difference approximations to differential conservation laws which themselves are in discrete conservation form. We now describe this class and for the sake of simplicity we do it in only one space variable.

Let the differential conservation law be

$$U_t = F_x \quad \text{where } F = F(U) ,$$

with initial conditions $U(x,0) = \phi(x)$. Let g be a function of 2 ℓ arguments which has the property that

$$(41) \quad g(U, \dots, U) = F(U).$$

Consider the following difference approximation to the equation $U_t = F_x$:

$$(42) \quad \Delta v / \Delta t = \Delta g / \Delta x$$

where

$$(43) \quad \Delta v = v(x, t + \Delta t) - v(x, t) , \quad v(x, 0) = \phi(x)$$

and

$$(44) \quad \Delta g = g(x + \Delta x/2) - g(x - \Delta x/2)$$

with

$$(45) \quad g(x + \Delta x/2) = g(v_{-l+1}, v_{-l+2}, \dots, v_l)$$

where the v 's are at points distributed symmetrically around $x + \Delta x/2$.

Multiply equation (42) by a smooth test vector of compact support, integrate with respect to x and sum over all values of t which are integer multiples of Δt . On the left side apply summation by parts, on the right side replace the variables of integration by $x + \Delta x/2$ and $x - \Delta x/2$ in the two integrals which appear there. If $g(x)$ is defined at non-mesh points by linear interpolation from $g(x + \Delta x/2)$ and $g(x - \Delta x/2)$; we get:

$$(46) \quad - \sum \int \frac{w(x, t) - w(x, t - \Delta t)}{\Delta t} v(x, t) dx \Delta t - \int w(x, 0) \phi(x) dx \\ = - \sum \int \frac{w(x + \Delta x/2) - w(x - \Delta x/2)}{\Delta x} g(x) dx \Delta t .$$

This leads to the following Lax-Wendroff

Consistency Theorem. Let v be the solution of the difference equation (42) in conservation form with initial conditions ϕ and suppose that as $\Delta t, \Delta x \rightarrow 0$ v tends boundedly almost everywhere to some limit U . Then U is a solution of the differential conservation law and has initial values ϕ .

This consistency theorem is actually central to the way that we are computing the shocked flow. We already know that solutions to the integral equation

$$(47) \quad \iint (w_t U - w_x F) \, dx \, dt + \int w(x, 0) \phi(x) \, dx = 0$$

satisfy the differential equations, the initial conditions, and the shock conditions. The consistency theorem says that solutions to (42) approximate the solutions to (47) near the shock as well as in the smooth region. Then, to compute shocked flows we merely have to iterate flow quantities using an equation of the class defined by (42).

We show now that if we apply smoothing to solutions of difference equations in conservation form, the smoothed functions also satisfy difference equations in conservation form. More precisely:

Smoothing Theorem. If a difference scheme satisfies a conservation law, and if smoothing is done by adding a term which is a first difference of a function S which has the two properties:

- 1) $S = S(U_{-\ell}, U_{-\ell+1}, \dots, U_{\ell-1})$
- 2) $S(U, U, \dots, U) = 0$

Then the scheme with smoothing also satisfies the same conservation law.

The proof follows simply by constructing

$$g_1(x-\Delta x/2) = g(U_{-\ell}, U_{-\ell+1}, \dots, U_{\ell-1}) + S(U_{-\ell+1}, \dots, U_{\ell}).$$

and using the difference scheme:

$$\frac{\Delta v}{\Delta t} = \frac{\Delta g_1}{\Delta x}.$$

It is clear from the definition of S that $g_1(U, U, \dots, U) = F(U)$ implying that the consistency theorem holds for g_1 as well as for g .

Such smoothing has been used by Kasahara [21] in atmospheric fluid dynamics problems and by Rusanov [22] in a variety of time-dependent problems. Kasahara reported that he used second order smoothing once every forty cycles to maintain stability instead of third order smoothing at each step as in this report. We tried a calculation in which we smoothed at alternate cycles. It became unstable very quickly.

In this section we have explained the reasons for using smoothing. We have shown that the smoothing retains all the accuracy that the original system had and that consistency in the sense of the integral operator is also preserved. In the next section the results of a machine computation at Mach 6. will be discussed.

VI. Computation.

A. Test Case.

The flow chosen for a test case was one computed by Eva Swenson and reported by her in [6]. This flow had plane symmetry and included a detached shock whose shape was prescribed to be

$$x = 3 \sqrt{1 + y^2}$$

where x is the distance along the axis of symmetry and y is the distance from the axis of symmetry.

The gas was assumed to be perfect with $\gamma = 1.4$. The Mach number at ∞ was 6. This inverse problem was solved to five figures of accuracy by Garabadian's method of characteristics in complex space [19], furnishing the body used in our calculation.*

B. Initial Flow.

Our time dependent method requires initial values of the flow quantities at interior points as well as at the body points. The choice of this initial flow is to a certain extent arbitrary. Presumably, the flow will eventually settle down to the correct steady state no matter what data one starts with. Of course, the closer

* Since the position of the body was not known at precisely the points needed by our finite difference method, we used quadratic interpolation to obtain the needed values.

our initial guess comes to representing the stationary flow, the faster it will converge to a steady state. In our calculation the initial data at the body were the results computed by Swenson; those at the upstream boundary were assigned the data at ∞ . The initial flow quantities at all other points were arbitrarily set to be linear functions of ξ , having the above data at the body and at the left boundary.

It was noticed that with initial data in which the pressure and density at the body were set equal to their values at ∞ , the calculational scheme became unstable after a few cycles. A possible explanation for this instability is that these initial values are too far from the steady state solution and initially give rise to too violent a flow. A similar difficulty was encountered by Burstein [11]. A way out of the difficulty was to iterate a number of cycles using only the first step of the two step method. This procedure is known to be stable. These numerical results indicate that if fluxes are too large, the two step method is unstable. This is an instance of nonlinear instability because for linear systems, stability is not influenced by the size of the initial data. At present, I know of no explanation for this instability nor for the subsequent stability of the scheme when applied to the more accurate data.

The usual stability analysis based on v. Neumann criteria is not applicable here because in that theory one has to assume that flow quantities at neighboring lattice points differ by $O(h)$, whereas in our calculation this instability occurred in the shock region where the flow quantities vary rapidly.

C. Verifications.

In this section we compare the results of our calculation with the exact steady state known from E. Swenson's work. We also present various flow quantities as functions of time.

1. Bernoulli Steady State Constant.

In [1, p. 300] it is proven that for a steady flow the quantity

$$B = (u^2 + v^2)/2 + 1/(\gamma - 1) \cdot c^2$$

is a constant along every streamline even when the streamline crosses a shock. Since each streamline comes from upstream, B is a constant throughout. The initial average of B is 29.04. The final average of B is 28.55. The correct upstream value is 28.700. The average of B as a function of cycle number is plotted on graph G1.

2. Stagnation Point Pressure.

The graph G2 illustrates the pressure at the stagnation point as a function of cycle number. The pressure at cycle number 0 is the steady state theoretical pressure p^* consistent with the parameters of the problem. Referring to the graph, it is seen that the pressure, which starts out at p^* , drops very rapidly, then turns around, overshoots p^* and finally approaches it asymptotically.

3. Standoff Distance of the Shock as a Function of Time.

The equations of motion assume that the gas appearing in the computation is a "gamma law" gas, that is that

$$p = A\rho^\gamma$$

where A is a function of entropy S alone. Specifically [1, p. 10]

$$A = ke^{gS} \quad (= 1. \text{ upstream})$$

where k and g are positive constants. Thus A is a monotonic increasing function of S and can be used as a measure of the entropy jump across the shock. Using this quantity, a simple method for determining the position of the shock would be to march from in front of the shock (the constant region) along a horizontal line until a point is reached at which A is greater than 1 and to assign the position of

the shock to that point. Unfortunately, due to oscillation of the flow quantities, the quantity A oscillates below 1, then above; then sometimes the cycle repeats. Because of these irregularities, the position of the shock is taken to be halfway between the last point of an unbroken sequence of points at which $A = 1$ and the first point of an unbroken sequence of points with $A > 1$. The position of the shock on the line of symmetry is graphed in G3 using this method, along with its theoretical position in units of meshpoints from the body. The position of the shock starts at 61.5, then it moves lower and finally returns to a position around 37.5. The true position is 44 in these units. The body is at 0.

4. Pressure Profile on the Body.

In graph G4, the pressure profile along the body is illustrated at three different times and the pressure curve obtained by interpolation from [6] is plotted on the same graph. As can be seen there, the pressure profile on the body at 100 cycles moves far below its exact position; then at 300 cycles far above, then comes much closer to theoretical results at 1000 cycles. The pressure near the nose of the body (lower point number) is relatively more accurate than it is downstream.

5. Final Shape of the Shock.

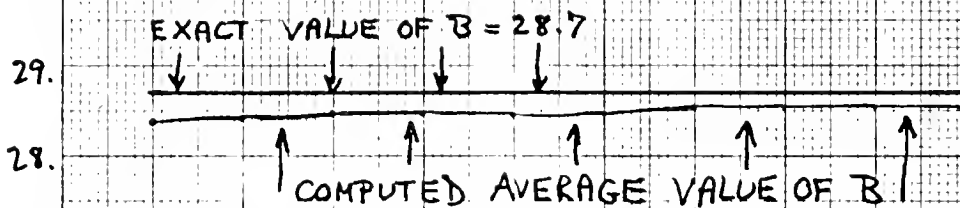
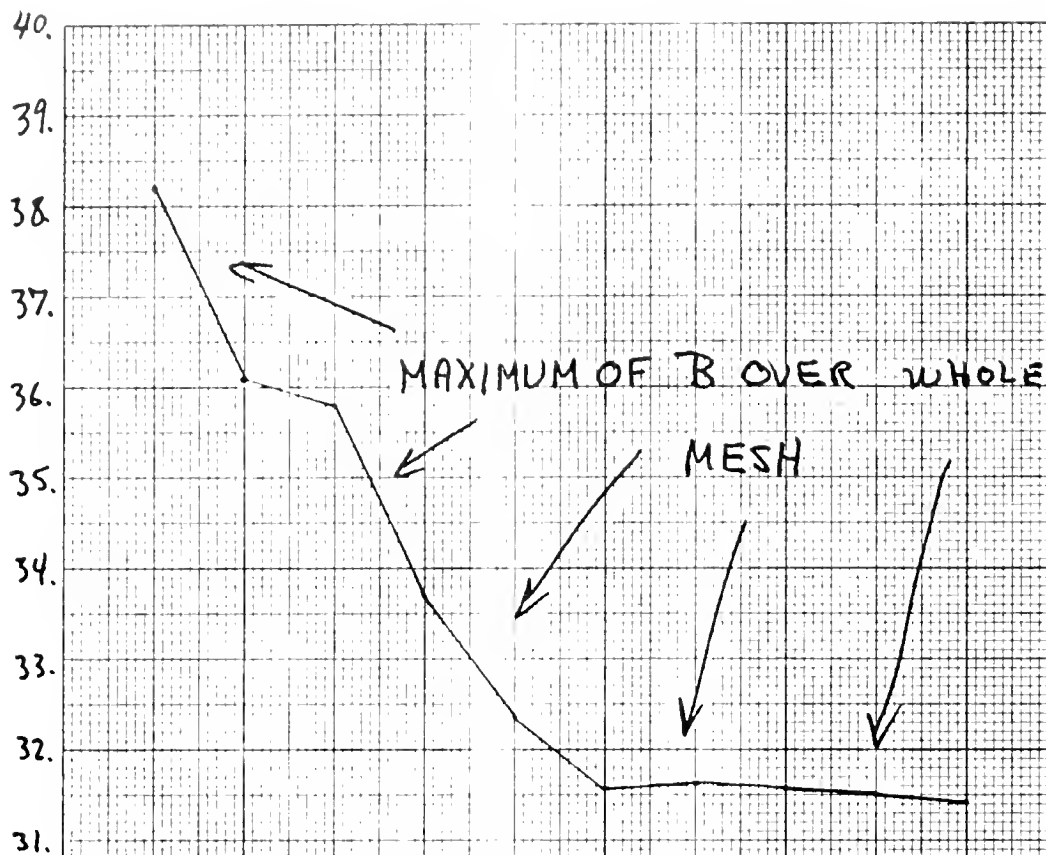
In graph G5, the position of the shock at 1000 cycles is illustrated and compared with its exact position and the position of the shock obtained using a finite difference analogue of equation (29). It is clear that the conservation analogue gives much better results than equation (29) especially near the upper boundary.

6. Summary.

In summary, the shape of the shock is close to the exact shape and the computed stagnation pressure is very close to its theoretical value. The shape of the computed pressure profile is close to the shape of the theoretical one although the values of pressure are up to 30% in error. These results are much better than those obtained from the non-conservative calculation in which the position of the shock deteriorated as $h'(y)$ became large and in which the shape of the pressure profile differed drastically from its theoretical shape.

In the future, we will make use of conservation laws and their conservative analogues as well as artificial viscosity and space transformations in truly non-stationary shock wave problems.

The author wishes to express his appreciation to Prof. Peter D. Lax for numerous helpful suggestions; to Prof. Robert D. Richtmyer for an introduction to the challenging scientific area of fluid dynamics computations; and to Prof. Max Goldstein for his cooperation in using the computing center at the Courant Institute of Mathematical Sciences. Thanks are also due to Prof. Samuel Burstein for a few short and stimulating discussions, and to Prof. Eva Swenson for graciously communicating the results of her own investigations into detached shock calculations.



$$B = \frac{u^2 + v^2}{2} + \frac{c^2}{8-1}$$

VS.

Cycle Number

100 200 300 400 500 600 700 800 900 1000

CYCLE NUMBER

55.

50.

45.

40.

35.

30.

25.

20.

15.

PRESSURE AT STAGNATION
POINT VS. CYCLE NUMBER

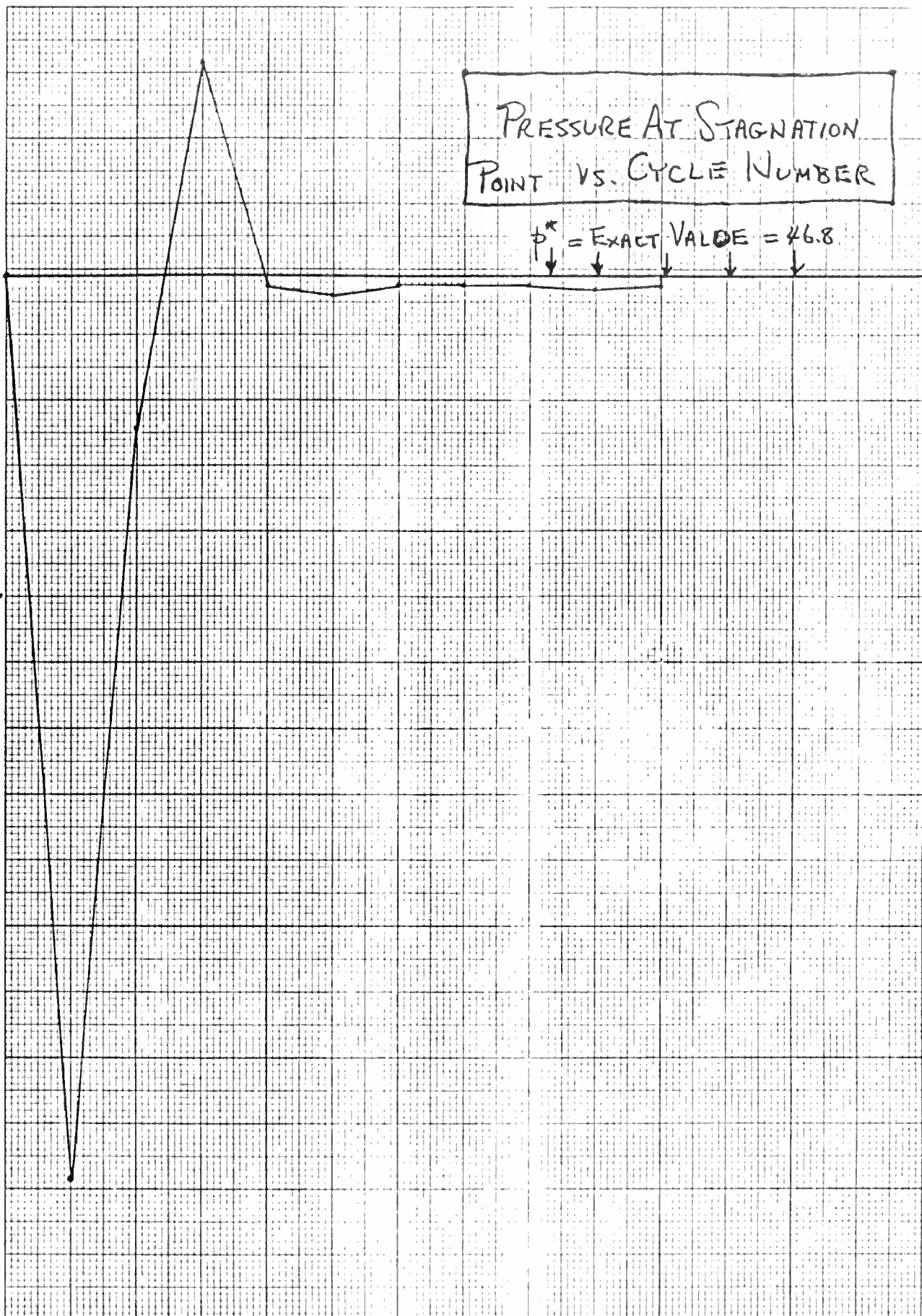
$p^* = \text{EXACT VALUE} = 46.8$

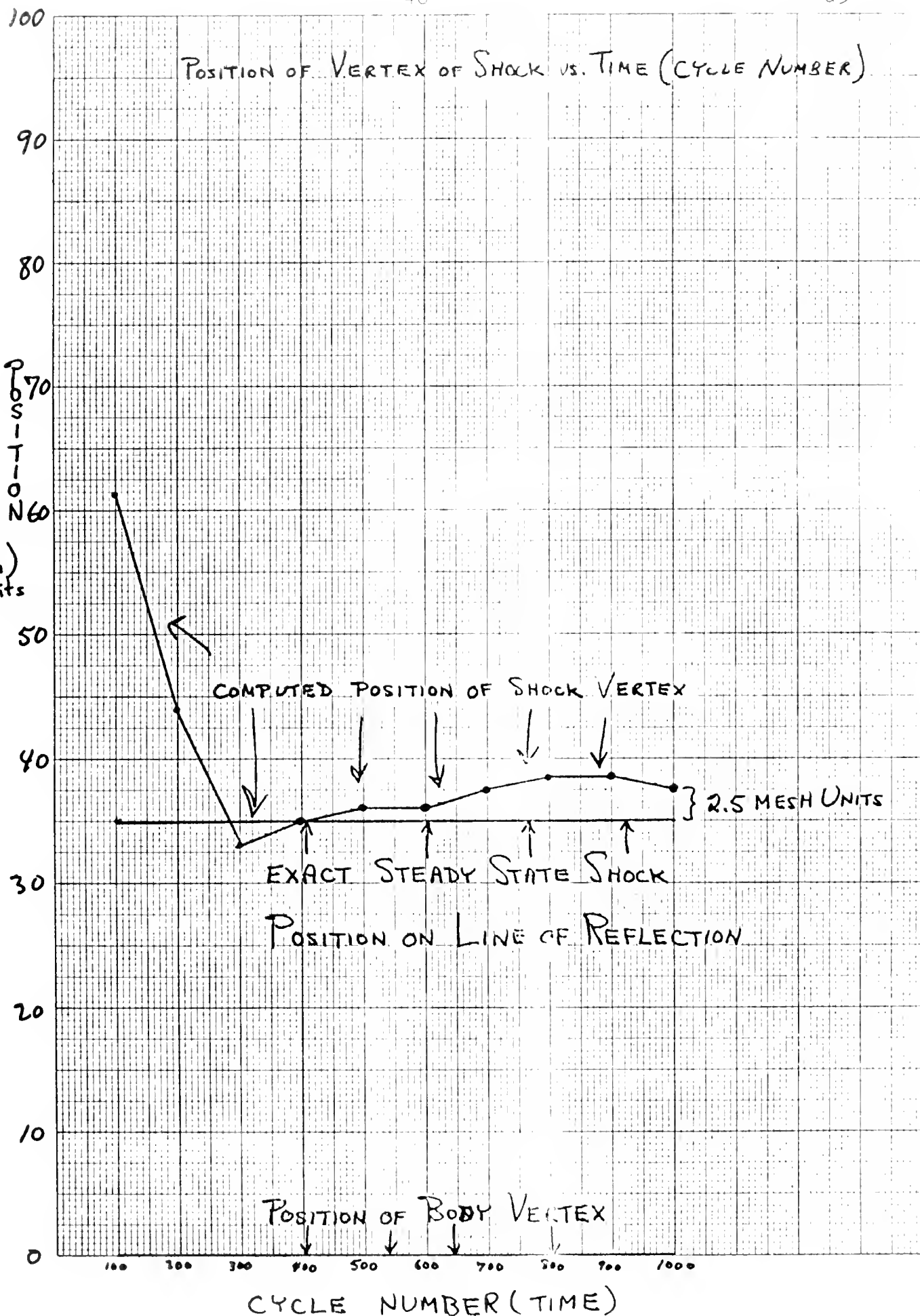
EUGENE DIETZGEN CO.
MADE IN U. S. A.

Pressure

NO. 341-20 DIETZGEN GRAPH PAPER
20 X 20 PER INCH

0 100 200 300 400 500 600 700 800 900 1000
CYCLE NUMBER



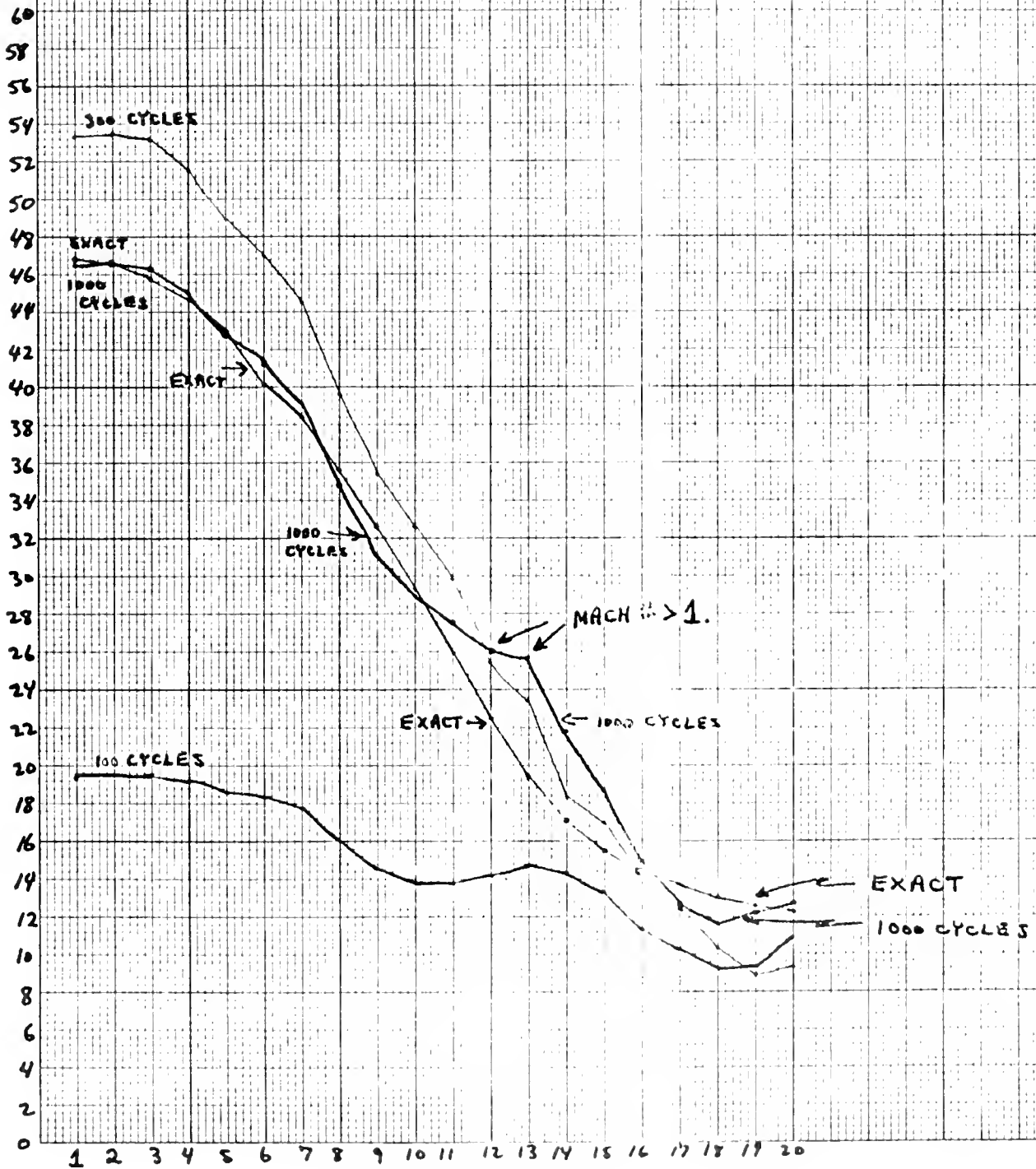
MADE IN U. S. A.
20 X 20 PER INCH

PRESSURE VS. γ
ALONG BODY

$P \uparrow$

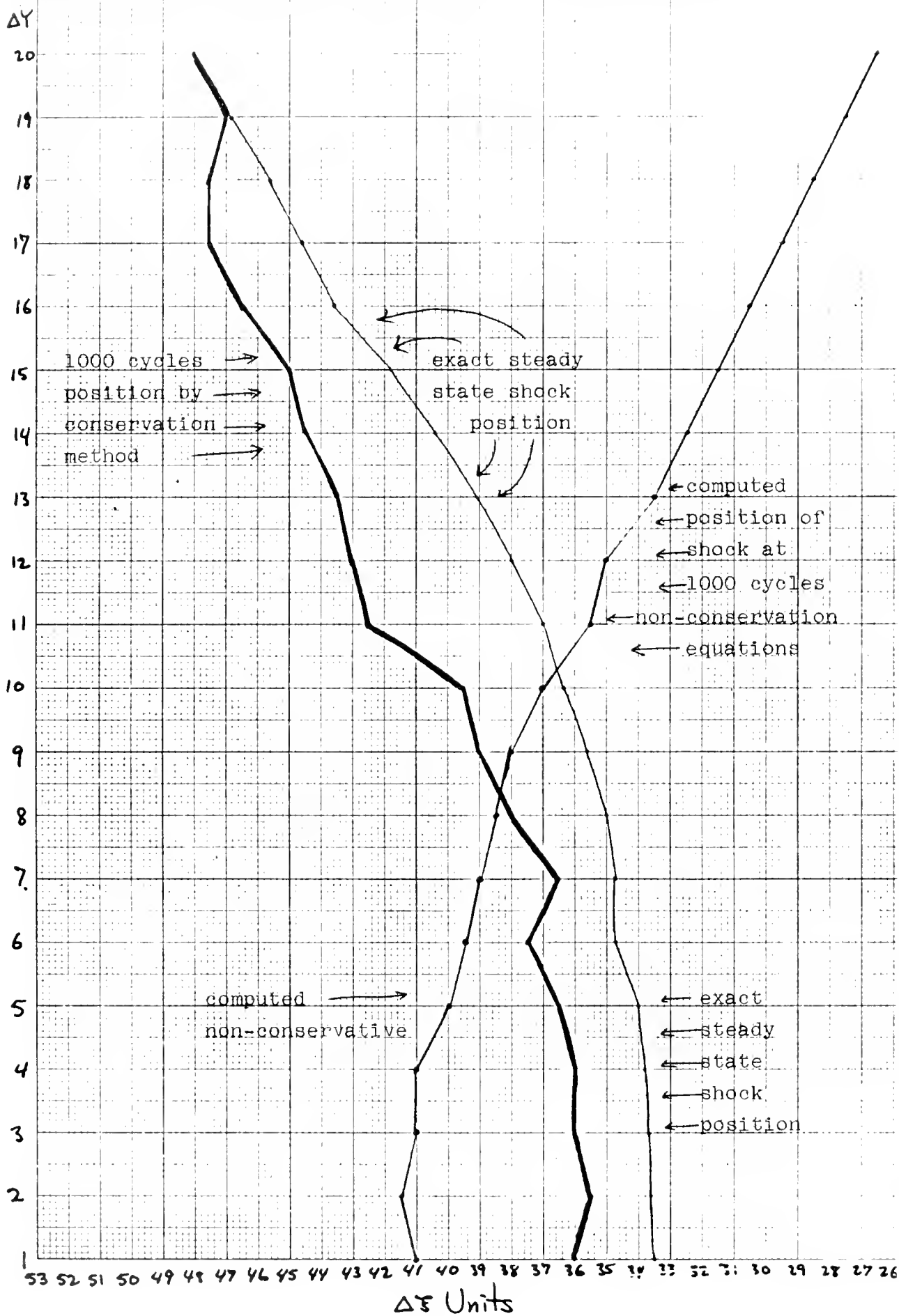
EUGENE DIETZGEN CO.
MADE IN U. S. A.

NO. 341-20 DIETZGEN GRAPH PAPER
20 X 20 PER INCH



EUGENE DIETZEN CO.
MADE IN U. S. A.

NO. 341-20 DIETZEN GRAPH PAPER
20 X 20 PER INCH



Bibliography

1. R. Courant and K. O. Friedrichs, "Supersonic Flow and Shock Waves" (Pure Appl. Math., Vol. 1). New York: Interscience, 1948.
2. P. R. Garabedian, Partial Differential Equations. John Wiley + Sons, 1964.
3. R. D. Richtmyer, "Proposed Fluid Dynamics Research." Unpublished Memorandum, Courant Inst. Math. Sci., New York Univ., Sept. 1960.
4. R. D. Richtmyer, "A Survey of Difference Methods for Non-Steady Gas Dynamics," NCAR Technical Note 63-2, 1963.
5. P. D. Lax and B. Wendroff, "Systems of Conservation Laws," Comm. Pure Appl. Math., Vol. 13, 1960.
6. E. V. Swenson, "Numerical Computation of Hypersonic Flow Past a Two-Dimensional Blunt Body," AEC Research and Development Report, NYO-1480-1, Courant Inst. Math. Sci., NYU.
7. G. E. Lewis, "Two Methods Using Power Series for Solving Analytic Initial Value Problems." AEC Research and Development Report, NYO-2881, 1960, Courant Inst. of Math. Sci., NYU.
8. S. Z. Burstein, "Finite Difference Calculations for Hydrodynamic Flows Containing Discontinuities. AEC Research and Development Report TID-4500, 43rd Ed., Sept. 1965.

9. O. M. Belotserkovskii, "On the Calculation of Flow Past Axisymmetric Bodies with Detached Shock Waves Using an Electronic Computing Machine," Jour. Appl. Math. Mech., Vol. 24, 1960.
10. D. Quarles, "A Moving Coordinate Method for Shock Wave Calculations -- Stability Theory Including Shock Boundary Conditions," Doctoral Dissertation, New York Univ., Oct. 1964.
11. S. Z. Burstein, Private Communication, New York.
12. R. Courant and D. Hilbert, Methods of Mathematical Physics, Vol. II., Interscience Publishers, New York, 1961.
13. A. E. Taylor, Advanced Calculus, Ginn and Co., New York, 1955, p. 462.
14. Milton Van Dyke, "The Supersonic Blunt-Body Problem-- Review and Extension," Jour. of the Aero/Space Sci., Vol. 25, 1958, p. 485.
15. Martha W. Evans and Francis H. Harlow, "Calculation of Unsteady Supersonic Flow Past a Circular Cylinder," ARS Journal, January, 1959.
16. Rusanov, V. V. Brief Scientific Communication, Section 12 of Intl. Congress of Math., Moscow, 1966.
17. K. I. Babenko, G. P. Voskresenskii, A. N. Liubimov, V. V. Rusanov, "Spatial Flow around Smooth Bodies in Ideal Gases," Moscow, Izd. Nauk., 1964.

18. J. von Neumann and R. D. Richtmyer, "A Method for the Numerical Calculation of Hydrodynamic Shocks," J. Appl. Phys. 21, No. 3, 232-237, 1950.
19. P. R. Garabedian and H. M. Lieberstein, "On the Numerical Calculation of Detached Bow Shock Waves in Hypersonic Flow," J. of Aeronautical Sciences, p. 109 25 1958.
20. K. A. Bagrinovskii and S. K. Godunov, "Difference Schemes for Multidimensional Problems," Doklady Nauk SSSR, Vol. 115, No. 3, 1957, pp. 431-433.
Translated by Phyllis Fox into English.
21. D. Houghton, A. Kasahara, W. Washington, "Long Term Integration of the Barotropic Equations by the Lax-Wendroff Method," Monthly Weather Review, Vol. 94, No. 3, March 1966, pp. 141-150.
22. V. V. Rusanov, "The Calculation of the Interaction of Non-Stationary Shock Waves and Obstacles," USSR Computational Mathematics and Math. Phys., No. 2, 1962.

This report was prepared as an account of Government sponsored work. Neither the United States, nor the Commission, nor any person acting on behalf of the Commission:

- A. Makes any warranty or representation, express or implied, with respect to the accuracy, completeness, or usefulness of the information contained in this report, or that the use of any information, apparatus, method, or process disclosed in this report may not infringe privately owned rights; or
- B. Assumes any liabilities with respect to the use of, or for damages resulting from the use of any information, apparatus, method, or process disclosed in this report.

As used in the above, "person acting on behalf of the Commission" includes any employee or contractor of the Commission, or employee of such contractor, to the extent that such employee or contractor of the Commission, or employee of such contractor prepares, disseminates, or provides access to, any information pursuant to his employment or contract with the Commission, or his employment with such contractor.

1. The first part of the paper is devoted to the study of the properties of the function $f(x)$ defined by the series $\sum_{n=0}^{\infty} a_n x^n$ where a_n are the coefficients of the series. The function $f(x)$ is shown to be analytic in the region $|x| < 1$ and to have a branch point at $x=1$. The function $f(x)$ is also shown to be bounded in the region $|x| < 1$ and to have a limit as $x \rightarrow 1^-$.

2. The second part of the paper is devoted to the study of the properties of the function $f(x)$ defined by the series $\sum_{n=0}^{\infty} a_n x^n$ where a_n are the coefficients of the series. The function $f(x)$ is shown to be analytic in the region $|x| < 1$ and to have a branch point at $x=1$. The function $f(x)$ is also shown to be bounded in the region $|x| < 1$ and to have a limit as $x \rightarrow 1^-$.

John Erdős

N.Y.U. Courant Institute of
Mathematical Sciences
251 Mercer St.
New York 12, N. Y.

